Opinion piece

THE ROYAL SOCIETY PUBLISHING

Applicability of drug response metrics for cancer studies using biomaterials

Elizabeth A. Brooks[1,†], Sualyneth Galarza[1,†], Maria F. Gencoglu[1,†], R. Chase Cornelison[2], Jennifer M. Munson[2] and Shelly R. Peyton[1]

[1]Department of Chemical Engineering, University of Massachusetts Amherst, 240 Thatcher Road, Amherst, MA 01003-9364, USA
[2]Department of Biomedical Engineering and Mechanics, Virginia Tech, 325 Stanger Street, Blacksburg, VA 24061, USA

SRP, 0000-0002-7364-8727

Bioengineers have built models of the tumour microenvironment (TME) in which to study cell–cell interactions, mechanisms of cancer growth and metastasis, and to test new therapies. These models allow researchers to culture cells in conditions that include features of the *in vivo* TME implicated in regulating cancer progression, such as extracellular matrix (ECM) stiffness, integrin binding to the ECM, immune and stromal cells, growth factor and cytokine depots, and a three-dimensional geometry more representative of the *in vivo* TME than tissue culture polystyrene (TCPS). These biomaterials could be particularly useful for drug screening applications to make better predictions of efficacy, offering better translation to preclinical models and clinical trials. However, it can be challenging to compare drug response reports across different biomaterial platforms in the current literature. This is, in part, a result of inconsistent reporting and improper use of drug response metrics, and vast differences in cell growth rates across a large variety of biomaterial designs. This study attempts to clarify the definitions of drug response measurements used in the field, and presents examples in which these measurements can and cannot be applied. We suggest as best practice to measure the growth rate of cells in the absence of drug, and follow our 'decision tree' when reporting drug response metrics.

This article is part of a discussion meeting issue 'Forces in cancer: interdisciplinary approaches in tumour mechanobiology'.

1. Introduction

Pharmacology metrics, such as IC_{50} (the inhibition concentration of a drug where the response is reduced by half), EC_{50} (the effective concentration of a drug that gives half-maximal response) and E_{max} (the drug's maximum effect), have been used to evaluate the results of drug response assays and describe drug potency. Recently, Hafner *et al.* [1] defined the GR_{50}: the concentration of a drug that reduces cell growth rate by half. The GR_{50} is an important contribution to the field of drug screening, because it accounts for the variable differences in growth rates between different cell lines. However, drug response metrics can be misrepresented or applied incorrectly in certain instances, which has led to inconsistent results between studies. One high-profile study, Haibe-Kains *et al.* [2], reported inconsistencies between two large pharmacogenomic studies: the Cancer Genome Project (CGP) [3] and the Cancer Cell Line Encyclopedia (CCLE) [4]. They compared the IC_{50} and the area under the dose–response curve (AUC) for 15 drugs across 471 cell lines, and found very little correlation between the two studies (Spearman's rank correlation of 0.28 and 0.35 for IC_{50} and AUC, respectively) [2]. Discrepancies between these studies and others could be attributed to differences between experimental protocols (e.g. type and length of assay, cell culture substrate and medium used), method of dose–response analysis or because different laboratories use and apply these pharmacological metrics to their results differently.

This type of inconsistency has extended to bioengineering, where new biomaterial platforms have been developed to incorporate features of the tumour microenvironment (TME), e.g. geometries, coculture systems and tunable extracellular matrix (ECM) stiffness. Bioengineers have postulated that these ECM cues from the TME could radically impact drug responses, which could be important for predicting the efficacy of a drug before embarking on preclinical studies. During a search of the literature, we observed that bioengineers have quantified drug responses using many different drug response metrics; however, it is not clear in every study why certain reporting tools were used, and whether or not they were applied correctly. As examples, we found cases where an IC_{50} was reported, but the drug was not effective enough to inhibit growth of half the cell population. Particularly a consideration when using different types of biomaterials, cell growth rate differences between two-dimensional (2D) and three-dimensional (3D) systems raises the question of whether the same metric tool should be used for both.

When analysing the literature, we wondered whether the implementation of a global, consistent analysis could reduce the disagreement of values reported. Could methods used to analyse drug responses in 2D culture also apply for 3D systems? In the case of coculture systems, should a different approach be used to separate the responses from cancer cells and healthy cells in the TME? With this in mind, this perspective paper compares select cases in the literature, our own data for cell responses to drugs in and on biomaterials, metrics reported and inconsistencies between studies. We end with a recommendation for the incorporation of additional drug response metrics when working with biomaterial systems.

2. Definitions of drug response metrics

Drug response assays evaluate the impact of a drug on a population of cells over a range of concentrations. For simplicity, we will define the number of cells at the start of the assay readout, or the 'initial value' of the cells, as y_0 (figure 1a). Unfortunately, many studies do not report y_0, which prevents some metrics from being reported, as we discuss later in this section. The cells are then incubated with drug for a defined period of time (typically 24–72 h), and cell viability is measured (y_{final}). Cells are also incubated with a small amount of the vehicle in which the drug was dissolved (often DMSO or water), serving as a control (y_{ctrl}). A drug is considered cytostatic if it slows or completely prevents growth of cells [5]. In other words, if the measured cell viability is between y_0 and y_{ctrl}, that drug is said to be cytostatic at that concentration. Cytotoxic means that the drug reduces the cell number below the initial cell count ($y_{final} < y_0$). Note that when y_0 is not measured, a true drug cytotoxicity cannot be reported.

There are six typical metrics used to report the effect of a drug on a cell culture: IC_{50}, EC_{50}, GI_{50}, GR_{50}, E_{max} and AUC (figure 1a). Figure 1 gives definitions of these metrics, with three hypothetical drug response curves with varying degrees of 'potency'. A 'potent' drug is 100% cytotoxic, a 'moderately potent' drug achieves 100% growth inhibition but no net cell death and a 'less potent' drug reduces cell growth by 50% (figure 1b−g). Drug potency can also be evaluated by the curve response class classifier (CRC), as described by Inglese et al. [6]. The CRC metric helps group the efficacy of cell and drug combinations to reveal if a particular combination is fully cytotoxic or cytostatic, and can be valuable in cases where a full dose−response curve is not obtained. Furthermore, these classifications aid in determining promising cases to select for future screening studies.

The IC_{50} and E_{max} metrics do not consider the initial population (y_0), nor the number of cell divisions during the length of the assay, which was a motivating factor for Hafner et al. [1] to define the GR_{50}. Only the GI_{50} and GR_{50} take y_0 into consideration. GI_{50} is the dose that inhibits the growth of cells by 50%, and GR_{50} represents inhibition of the growth rate, not total growth, of the cell culture. The initial cell population, y_0, can vary between type of assay, cell type or length of assay. To account for this variation, GR_{50} is represented as data normalized with respect to the initial values (figure 1e−g).

Although the '50' in IC_{50}, EC_{50}, GI_{50} and GR_{50} metrics signifies a 50% inhibition, they can be used with values other than 50 to indicate different effects, e.g. IC_{90} [7,8]. Negative values can be used for the cytotoxic regime ($y_{final} < y_0$), although these do not come from the formal definitions of GI or GR. In this case, GI_{10} would be the concentration where the cells are reduced 10% from the initial value ($y_{final} = 0.9 \times y_0$), and GI_{-100} would be the concentration which kills all the cells. In the figure 1 example, 0–100 is defined over the range of $20\,k \le y \le 100\,k$, while -100 to 0 is defined over the range of $0 \le y \le 20\,k$. IC_{-n} or EC_{-n} values are not possible since these metrics do not consider initial values.

The E_{max} represents the maximum and the AUC metric represents the cumulative effect of the drug. E_{max} is the fraction of viable cells at the highest drug concentration tested in the experiment, and AUC is the area under the viability curve for a cell population over the tested drug concentration range. Although neither of these metrics make any explicit assumption about growth kinetics, they still depend on the concentration range, experiment duration and cell growth rate, which means that their reported values cannot be compared with other studies in most cases. Fallahi-Sichani et al. [9] found AUC to be a robust response metric when the goal was to compare a single drug across identical cell lines. However, these need to be exposed to identical dose ranges, and preferentially at an intermediate concentration. E_{max} can be used with multiple drugs and concentration ranges but is more informative at high doses [9]. Particularly, in the case of E_{max}, Fallahi-Sichani et al.'s work highlighted it as a parameter that yielded high variation independent of cell proliferation rate. Yet, this study was unable to conclude what drug metric parameter best describes a drug response without considering drug concentration.

The IC_{50} is the most commonly reported drug response metric [10] and, therefore, it is important to highlight cases in which it is used with an incorrect definition. For instance, the IC_{50} should not be considered a measure of cell death [5]. As one example, in a case when the control value is more than 200% of the initial value ($y_{ctrl} > 2 \times y_0$, as can be seen in the examples given in figure 1b−d), the IC_{50} will result in a 'cytostatic' dose, but the cells are still growing, be it at a reduced rate. Second, in a case where a reduction in half the population is not reached (such as in [11–13]), the IC_{50} cannot be appropriately calculated, and instead the EC_{50} is the more appropriate metric to report. In other instances in the literature, the EC_{50} and GI_{50} are confused with the IC_{50} [1]. However, the GI_{50}

(a) E_{max}: the maximum level of growth inhibition or cell death possible with the drug
area under the curve (AUC): the area under the curve fitted to the drug-response data

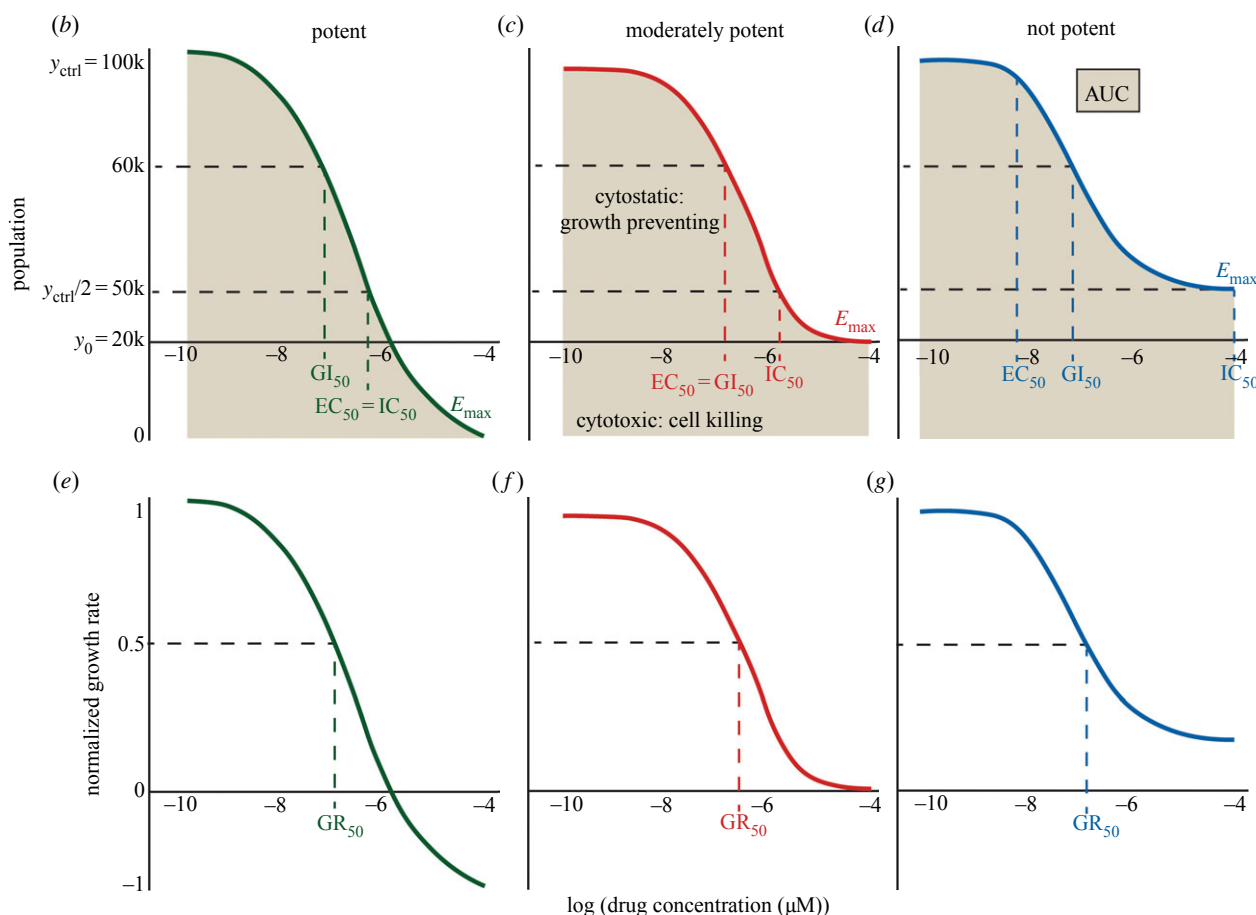| metric	the drug concentration which …	the drug concentration where …
IC_{50}	reduces population to half of the control value	$(\text{population}) = 0.5 \times y_{ctrl}$
GI_{50}	reduces total cell growth by 50%	$(\text{population}) = \dfrac{(y_{ctrl} - y_o)}{2} + y_o$
GR_{50}	cell growth rate inhibited by 50%	$(\text{population}) = 2^{\log_2 (y_{GI50}/y_o)/(y_{GI50}/y_o)} - 1$
EC_{50}	achieves half of the effect defined by E_{max}	$(\text{population}) = \dfrac{(y_{ctrl} - E_{max})}{2} + E_{max}$

Figure 1. Definitions and examples of drug response metrics. The IC_{50} represents the drug concentration where the response is reduced by half. The EC_{50} represents the concentration of a drug that gives half-maximal response. The GI_{50} represents the concentration of a drug that reduces total cell growth by 50%. The GR_{50} represents the concentration of a drug that reduces cell growth rate by 50%. The E_{max} represents the fraction of viable cells at the highest drug concentration (maximal response), and the AUC represents the area under the dose–response curve. The y-axis shows the cell count (top plots) and normalized growth rate (bottom plots). Drugs are considered 'cytotoxic' if viability is reduced below the initial value (y_0), and 'cytostatic' if viability is above the initial value, but below the control value (y_{ctrl}). Right curves (less potent) show a drug which reduces viability by 50% at maximum dose (IC_{50} is the maximum dose). Middle curves (moderately potent) show a drug which completely inhibits growth, but is not cytotoxic (E_{max} = initial viability). Left curves (potent) show a drug which is 100% cytotoxic (E_{max} = 0). Note that in these special cases, some of the other metrics are also equal to each other, which are labelled on the plot. (Online version in colour.)

metric is a correction of the IC_{50}, since it takes into consideration the initial cell count (y_0) [14,15].

Through our analysis, we also found examples where authors report a GI_{50}, when it is actually an IC_{50} (they did not measure y_0) [16]. For example, the cell population could grow over the course of an experiment, while the measured population values could still be lower than the control. Therefore, the initial cell populations must be measured to know whether a drug is killing cells or only slowing their growth. In addition, the IC_{50} is sometimes discussed in the context of growth inhibition [17], although it is not capable of measuring this. We thus recommend the field report the metric that is most appropriate for their observed responses

and experimental conditions, given the explanations stated above. We also recommend that researchers measure the initial cell population values (y_0), which will enable them to calculate GI_{50} and GR_{50} (if cell growth of the control is achieved over the course of the assay), particularly important where multiple cell lines or growth conditions are being tested as these metrics will account for differences in growth rates. This is also the only way to know if a drug is truly cytotoxic, as we mentioned earlier.

The GR_{50} is very similar to GI_{50}, but is defined by reduction in the growth rate, not cell growth as the GI_{50}. Growth rate inhibition is calculated from initial and control values, and the fitting for the GR_{50} relies on the assumption

that the cells are in exponential growth before application of the drug. GR_{50} is thus reported to be more robust than GI_{50} against variations in experimental protocols and conditions [1].

3. Applying drug response metrics to data obtained from biomaterial drug screening assays

Drug screening with cells on biomaterials rather than on tissue culture polystyrene (TCPS) is increasingly popular due to the ability to capture more physiologically relevant features in biomaterials that may impact drug response. Two-dimensional [18–20] and 3D [11,21,22] biomaterial platforms have been developed to study cell behaviour *in vitro*. Since it is widely accepted that cells grow at different rates in 2D and 3D biomaterial platforms [23], it is difficult to compare drug responses across these different environments without a GI_{50} or GR_{50}. Experiments to obtain these metrics require only minor adjustments to traditional drug screening protocols performed by seeding cells in an additional plate to measure initial population values (y_0) (figure 2a). In particular, the GR_{50} has worked very well for over 4000 combinations of breast cancer cell lines and drugs on TCPS [24], but has only been used in 3D biomaterials in limited reports [25].

Our own laboratory uses both 2D and 3D biomaterials in addition to TCPS for drug screening studies [26,27], and we have adapted our experimental procedures to collect data for calculating GR metrics in addition to the other metrics depicted in figure 1. However, we have found that the GR_{50} cannot always be applied. As it has been previously reported [1,24], it is necessary for the cells to achieve exponential growth over the course of the assay to use the GR_{50}. On TCPS, this is not an issue, as demonstrated by our data in figure 2b with SKOV-3 ovarian cancer cells dosed with paclitaxel. In this case, the GR values span a -1 to 1 range, which results in a good curve fit to calculate a GR_{50}.

Another important factor to consider in preclinical drug screening assays is the increasing use of patient-derived primary cells. This has become a hurdle as many primary cells grow more slowly, or in some cases not at all, making it impossible to calculate a GR_{50} value. In these cases, the calculated GR values remain well below 0.5, even at a control dose. Therefore, the formula for calculating GR values can be applied, but with low growth rates the GR_{50} specifically does not apply (though the GR curve could still provide useful information). As illustrated by our own data of patient-derived cells—ovarian cancer cells from ascites dosed with cisplatin on TCPS (figure 2c)—IC_{50} and EC_{50} values could be calculated, but the growth rate was too slow for a GR_{50} value, and one could not be calculated. This serves as an example in which additional drug response metric parameters are necessary to understand the effect of drug dosing, given that these primary cells proliferated very slowly when grown in a 3D environment.

For example, work by Longati *et al.* [11] highlights how pluripotent stem cell (PSC) drug response differs on 2D versus in 3D biomaterials. Although IC_{50} values were not reported in this work, we calculated the IC_{50} and EC_{50} from their published data and observed higher resistance in their

PSC cells in 3D compared to 2D (electronic supplementary material, table S1). Ivanov *et al.* [22] performed drug response studies with neural stem cells (NSCs) and the UW228-3 glioblastoma cell line in 3D. They found that the NSC drug response was biphasic, but not for the human glioblastoma cell line (which showed more resistance in 3D). Here, two IC_{50} values were reported for the same curve in the case of primary cells, representing a situation where an IC_{50} (or GI/GR/ EC_{50}) is inappropriate. We would suggest an AUC or E_{max} instead, which are not dependent on curve fitting (figure 1b–d).

As demonstrated by our own experimental data (figure 2d), culture of 3D patient-derived ovarian carcinoma ascite spheroids (OCAS) from ascites in a non-degradable 3D hydrogel exhibited a low growth rate over the course of the assay. Although a drug response curve with mafosfamide was generated from the data (figure 2d), this does not mean that a valid GR_{50} value can be obtained. GR value curves need to pass through $GR = 0.5$ or they cannot have a reliable GR_{50} value, even if certain curve fitting software gives a value for these circumstances, as we demonstrate in figure 2d. Therefore, we recommend that only the online GR calculator [1] be used to calculate GR metrics from raw data to ensure that true GR metrics are reported. There are cases of drug screening in 3D environments [25] where the GR metrics could be applied, but since growth is often slower in 3D than in 2D, the application of the GR calculations should be done carefully. In contrast with our dosing of ovarian cancer cells above, we demonstrate in figure 2e an example where we encapsulated SKOV-3 cells grown in multicellular tumour spheroids (MCTS) in a 3D hydrogel and dosed with mafosfamide. In this case, the cell growth was high enough to calculate a GR_{50}. From our own work, we recommend reporting the GR_{50} when possible to best account for differences in growth rates between different cell sources. We also encourage others to provide all the raw data and drug response curves with their publications to allow others to compare published results with their own (electronic supplementary material, table S2).

To further characterize the drug response in different material environments, we applied CRC metrics described by Inglese *et al.* [6] to our own data (figure 2f). We found that the r^2 values that we obtained for the nonlinear curve fits to the data were less than 0.9, which meant it was not possible to fit our results into these exactly defined classes according to the criteria set by Inglese *et al.* However, some of these drugs had greater than 80% efficacy, and displayed drug response curve with one (partial), two (complete) or no asymptotes (incomplete). We found that the 3D models, OCAS in a 3D non-degradable hydrogel and SKOV-3 MCTS in a degradable 3D hydrogel, were in the same curve response class: 'partial' even though their GR metrics were very different. Additionally, patient cells on TCPS had a 'complete' response (class 1a), but it was not possible to calculate biologically meaningful GR metrics. Interestingly, at the range of concentrations that were tested, the case of SKOV-3 cells on TCPS was classified with an 'incomplete' response (class 2a), but all the traditional dose-response and GR metrics could be calculated. These additional metrics could be helpful for eliminating cases for further study in biomaterials when there are no responses (class 4), but we do not show any examples of that here. Characterization with CRC could be used as another method for grouping drug curve responses on biomaterials.
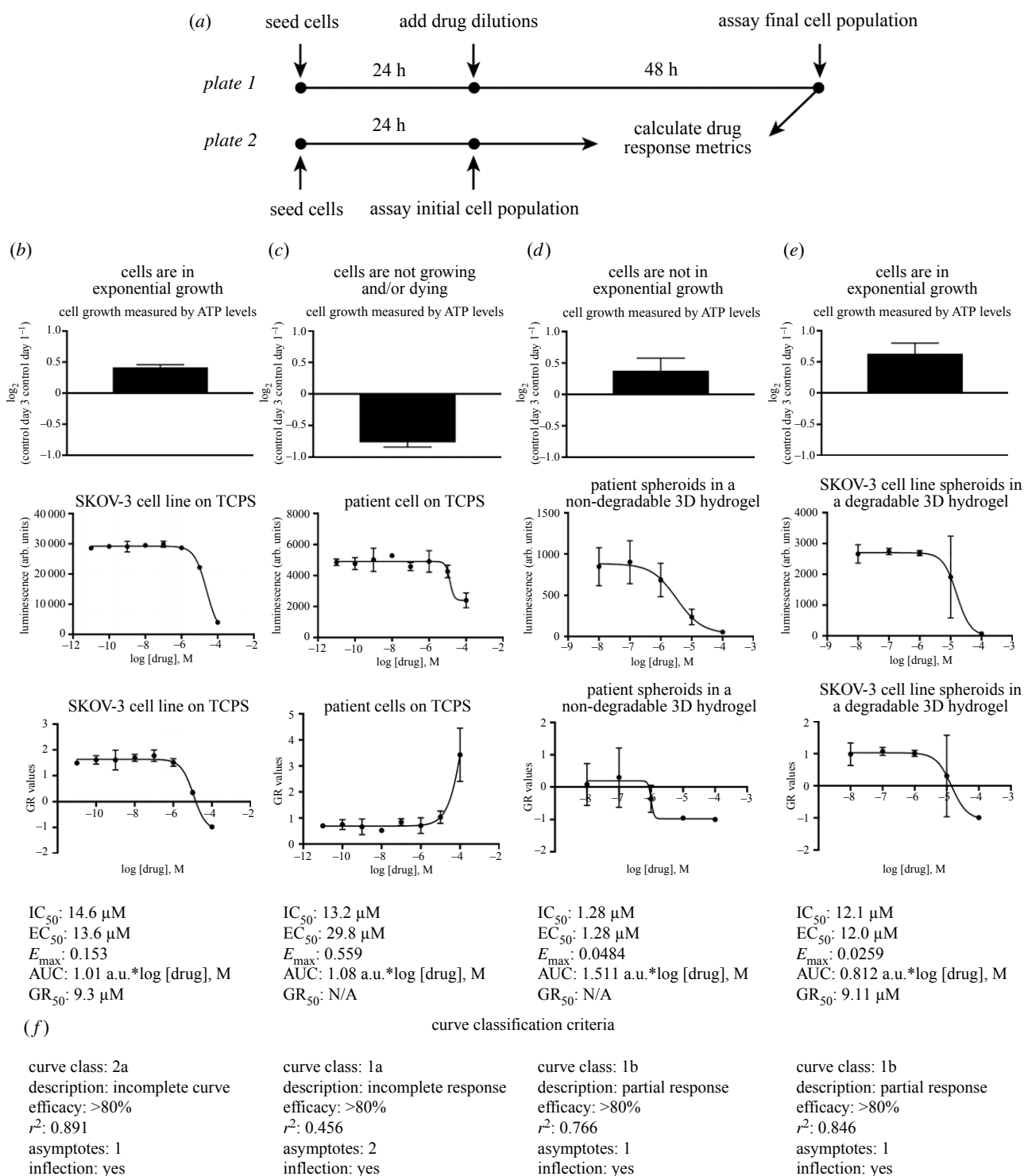
Figure 2. (a) Schematic of typical experimental work flow for a drug response assay. Cells are seeded on a 2D tissue culture plastic surface, on a 2D biomaterial or within a 3D biomaterial for drug dosing. Wells in a second plate are seeded with the same conditions as the drug dosing plate to measure GI_{50} or GR_{50} values. After 24 h, drugs are added to the drug dosing plate and the second plate for initial values is assayed simultaneously for initial cell counts. The drug dosed plate is incubated for a period of time (e.g. 48 h) and then assayed for the final cell response. The collected data is used to calculate drug response metrics. (b) Cells grown on tissue culture plastic achieve sufficient growth to generate a traditional dose-response curve, as well as a GR values curve to calculate a GR_{50}. (c) An example of patient cells grown on tissue culture plastic that do not grow exponentially over the course of the dosing assay. This results in a curve for traditional drug response metrics, but a GR curve cannot be calculated. (d) This is a case where cells grow over the course of the assay, but sufficient growth for calculating a GR_{50} measurement is not achieved because the resulting GR values are less than 0.5, which is the point where the GR_{50} is calculated. (e) Cell line MCTS encapsulated in a degradable 3D hydrogel demonstrates enough growth to calculate a GR_{50} and other drug response metrics. (f) Curve response classification descriptions for the data shown here. The cases presented here do not exactly correspond with the criteria described by Inglese et al. (particularly r^2 values), but we categorized them to their nearest classification.

4. Evaluation of drug responses in biomaterials reported in the literature

To compare IC_{50} values across studies, we mined data from 25 reports that performed drug screening with biomaterial systems, and that provided raw data that could be extracted and analysed independently. We calculated the IC_{50}, EC_{50}, E_{max} and AUC values and organized them by drug in electronic supplementary material, table S1. We were not able to calculate GI_{50} and GR_{50} because the initial population

(y_0) and control (y_{ctrl}) values were not provided in these studies. Table 1 shows a summary of the reported IC_{50} values from the literature and the drug response metrics calculated by us from their reported data. Table 2 summarizes cases where the drug response curve did not reach 50% inhibition, meaning the IC_{50} was not reached. Table 3 summarizes cases where the IC_{50} values reported in the literature did not agree with the values we calculated from reported data. We also applied the CRC metrics described by Inglese et al. [6] to the data we extracted from the literature (tables 1 and 3).

First, we found that for highly potent drug–cell line combinations, such as MCF7 with paclitaxel or MDA-MB-231 with epirubicin, IC_{50} values reported were in the same order of magnitude (table 1). By contrast, when a cell line was not particularly sensitive to the drug, like in the case of the MDA-MB-231 cell line to paclitaxel or docetaxel and MCF7 treatment with doxorubicin or tamoxifen, IC_{50} values reported from different studies varied much more strongly. This variance appears to be more dependent on the potency of the drug than the platform in which the cells were treated. When drug sensitivity was moderate or low, wide ranges in IC_{50} values tended to be even more drastic in the 3D models compared to 2D.

Another finding in table 1 is that highly efficacious drugs had 'complete' response curves, while less efficacious drugs had 'partial' or 'incomplete' curves. This is unsurprising, though there are some interesting observations: (i) all the drugs that failed to reach IC_{50} values had 'incomplete' curves; (ii) 'incomplete' or 'partial' response curves were mostly obtained in 2D models, while drugs tested in 3D models tended to display a 'complete' response curve. Paclitaxel results with MDA-MB-231 are a good example of this [20,27,38]. These results also illustrate the inadequacy of r^2. In table 1, we present five cases (out of 28 cases in table 1) where $r^2 > 0.9$, while the drug response curve had no asymptotes. So, it is unclear if Inglese et al.'s criteria apply here.

One of the major challenges we encountered during our literature search was that a limited number of studies published their drug response curves. Some publications did not report IC_{50} values for cases where the drug concentration did not kill half of the cell population (table 2). Unsurprisingly, these drug response curves were all 'incomplete', with one exception. In most cases, there were too few points to even calculate an r^2 value from the nonlinear fit. In these cases, r^2 was reported as 'ND' (non-determined).

Table 3 illustrates cases in which the IC_{50} we independently calculated did not agree with the one reported. This was mostly the case for cell lines that were fairly drug insensitive, as evidenced by the 'partial' response curves of these drugs. Despite the 'partial' response curve, E_{max}, IC_{50} and other metrics could be calculated for these drugs. This finding is significant, because it shows a pitfall of assessing drugs based on metrics without accounting for the drug response curve. The drugs in table 3 would seem efficacious based on their response metrics, although the raw response curves show that these cells are insensitive to these drugs. Finally, similar to table 1, the drug response curves in table 3 have r^2 values of greater than 0.9, but only one asymptote (partial). This again shows that r^2 alone is not an adequate criterion for CRC classification.

The drug response metric values reported in tables 1–3 vary by study, and may depend on the type/length of

assay, biomaterial used and/or analysis conducted. The most commonly used cell viability assays in our search included MTT assay [38], AlamarBlue (i.e. resazurin), Live/Dead staining and CellTiter-Glo. These types of assays indirectly measure the cytostatic or cytotoxic effect of a drug, via metabolic activity, counting of dead cells, cell death or ATP activity. There are additional complications with data reported in the literature. Many publications did not present enough data points for us to calculate IC_{50}, and could not be included in the comparison. There were other published reports where no metrics were reported, which makes it impossible to relate them to other published data. Clearly, better standard practices should be adopted. We recommend that future publications explicitly define the metrics they use, for two reasons. First, clearly explaining the metrics used in an article would help others learn about drug response metrics, and it would also prevent them from misinterpreting results. Second, definitions of the metrics are dependent on the context. For example, in the articles we summarized, 'inhibition' in IC_{50} refers to the inhibition of cell viability. In other works, however, it may refer to the inhibition of cell growth, which should be called a GI_{50} and calculated accordingly.

Among the 30 studies we examined, 25 presented drug response curves from which IC_{50} values could be obtained. We used the WebPlotDigitizer Tool (https://automeris.io/WebPlotDigitizer) [39] to extract drug concentrations and cell viabilities from these curves. These data were analysed in GraphPad Prism to calculate an IC_{50} using nonlinear regression with variable slope (four parameter) and least-squares fit method. From the data summarized in tables 1–3, we made comparisons between the 51 drug response curves and IC_{50} values reported in these studies. We found our results in agreement with 35 of these (69%), including five cases where neither we nor the original authors could obtain an IC_{50} value due to drug potencies being too low. In 16 cases (31%), IC_{50} values were significantly different between the value reported and our own calculation. These differences are possible because (i) we extracted the numerical data from plots in article figures, which may introduce error; (ii) different researchers may have used different forms of nonlinear regression (e.g. least-squares or robust fit methods for curve fitting, fixing the hill slope to the standard −1 or using variable slope); (iii) other researchers may have chosen different methods (appropriate or not) to handle problems such as outliers and negative inhibition, including setting constraints on the maximum and minimum values, manually determining outliers, using software algorithms for automatic outlier detection, etc.; and (iv) there could be cases where the IC_{50} could not be calculated due to the shape of the fitted curve, yet some data analysis software will attempt to calculate an IC_{50} that results in an unrealistic value.

5. Assessing drug response in coculture systems

Coculturing cancer cells with stromal cells (e.g. cancer-associated fibroblasts, pericytes or adipocytes) has been shown to drastically alter drug response, ranging from promoting drug resistance to increasing drug sensitivity [25,40–44]. Furthermore, multicellular cocultures may be more physiologically relevant than monocultures, either in 2D or 3D, as they can account for tissue-level interactions. In fact, it was

Table 1. Variation of IC$_{50}$ reported for cell line-drug responses in different publications. Note: partial response, 1 asymptote; incomplete, 0 asymptote; complete, 2 asymptotes.

drug	cell line	format	reported IC$_{50}$	IC$_{50}$ range reported	IC$_{50}$ range calculated	calculated						
						IC$_{50}$	E$_{max}$ (growth inhibition)	AUC	EC$_{50}$	R^2	curve	group
paclitaxel	MCF7	2D	0.003 μM	0.003–8.3 μM	0.003–0.009 μM	0.003 μM	78% @ 11 μM	224.70	0.004 μM	0.97	partial	[21]
		2D	3.2–8.3 μM			0.009 μM	71% @ 0.2 μM	156.40	0.006 μM	0.95	incomplete	[18]
		2D	—			10.9 nM	55% @ 500 nM	385.2	18 nM	0.96	partial	[28]
		3D GFR Matrigel	0.006 μM	ND–0.006 μM	0.0028–0.005 μM	0.005 μM	34% @ 191 μM	452.20	0.008 μM	0.97	partial	[21]
		3D PEG-heparin	—			2.81 nM	37% @ 500 nM	381.9	2.33 nM	0.91	complete	[28]
	MDA-MB-231	2D	0.004 μM	0.004–7.5 μM	0.002–4.6 μM	0.002 μM	97% @ 50 μM	139.60	0.004 μM	0.98	partial	[21]
		2D	—			17.97 nM	45% @ 500 nM	418.8	13.59 nM	0.86	partial	[28]
		2D	7.5 μM			4.6 μM	97% @ 25 μM	2.375	5.26 μM	0.89	incomplete	[29]
		3D GFR Matrigel	0.03 μM	0.03–50 μM	0.03–50.3 μM	0.03 μM	74% @ 199 μM	335.70	0.04 μM	1.00	complete	[21]
		3D PEG-heparin	—			4.41 nM	37% @ 500 nM	411.9	7.31 nM	0.94	complete	[28]
		3D fibroin silk	50 μM			50.3 μM	58% @ 60 μM	3.326	25 μM	0.98	incomplete	[29]
doxorubicin	MCF7	2D	0.23 μM	0.23–0.84 μM	0.3–0.88 μM	0.3 μM	100% @ 112 μM	340.60	0.3 μM	0.98	complete	[17]
		2D	0.84 μM			0.88 μM	99% @ 117 μM	249.6	0.66 μM	1.00	incomplete	[30]
		3D GFR Matrigel	could not be calculated	ND–70 μM	14.2–60 μM	14.2 μM	100% @ 239 μM	457.60	8.8 μM	1.00	partial	[17]
		3D Matrigel	EC$_{50}$ = 12			not reached	41% @ 4 μM	237.3	1.76 μM	1.00	incomplete	[31]
		3D agarose	70 μM			32.79 μg ml^{-1} (60 μM)	79% @ 115 μM	294.8	19 μM	1.00	partial	[30]
tamoxifen	MCF7	2D	7.74 μM	7.74–14 μM	7.11–7.443 μM	7.11 μM	80% @ 100 μM	81.47	4.9 μM	1.00	partial	[32]
		2D	14.0 μM			7.443 μM	99% @ 807 μM	163.6	14.49 μM	0.97	complete	[33]
		3D	20.62 μM	20.6–72.6 μM	21–71.35 μM	21 μM	58% @ 90 μM	126.4	14.4 μM	0.99	complete	[32]
		3D pNG cryogel	45.6 μM			45.09 μM	95% @ 800 μM	224.9	38.5 μM	0.99	complete	[33]
		3D polyNIPAM spheroids	72.6 μM			71.35 μM	88% @ 80 μM	235.9	39 μM	0.99	complete	[33]

(Continued.)

Table 1. (Continued.)

drug	cell line	format	reported IC$_{50}$	IC$_{50}$ range reported	IC$_{50}$ range calculated	calculated						
						IC$_{50}$	E$_{max}$ (growth inhibition)	AUC	EC$_{50}$	R^2	curve	group
epirubicin	MDA-MB-231	2D	0.05 μM	0.05–0.6 μM	0.04–0.49 μM	0.04 μM	100% @ 1.1 μM	204.30	0.03 μM	0.97	partial	[21]
		2D	0.6 μM			0.49 μM	85% @ 10 μM	287.7	0.41 μM	1.00	partial	[34]
		3D GFR Matrigel	0.58 μM	0.58–0.6 μM	0.3–0.5 μM	0.5 μM	100% @ 52 μM	282.20	0.3 μM	0.99	complete	[21]
		3D spheroid	0.6 μM			0.317 μM	70% @ 10 μM	285.3	0.28 μM	1.00	partial	[34]
docetaxel	MDA-MB-231	2D	0.2 μM	0.2–31.4 μM	0.065–35 μM	0.065 μM	73% @ 10 μM	247.4	0.05 μM	1.00	partial	[35]
		2D	31.4 μM			35 μM	93% @123 μM	297.9	25.12 μM	0.96	incomplete	[35]
		3D	10 μM	—	—	not reached	29% @ 0.1 μM	312.4	could not determine	0.88	incomplete	[34]

Table 2. Examples where IC$_{50}$ was not reached (drug concentration did not kill half the cells).

drug	cell line	format	reported	calculated						
				IC$_{50}$	E$_{max}$ (growth inhibition)	AUC	EC$_{50}$	R^2	curve	group
doxorubicin	MCF7	3D	EC$_{50}$ = 12 μM	drug did not kill half of the cells (IC$_{50}$ not reached)	41% @ 4 μM	237.3	1.76 μM	0.99	incomplete	[31]
methotrexate	JIMT1	2D	IC$_{50}$ not reported		30% @ 20 μM	406.80	0.02 μM	ND	incomplete	[12]
helenine	JIMT1	2D	IC$_{50}$ not reported		11% @ 20 μM	511.70	2.0 μM	ND	incomplete	[12]
API-2	JIMT1	2D	IC$_{50}$ not reported		17% @ 20 μM	398.70	11.1 μM	ND	incomplete	[11]
gemcitabine	BXPC3	3D	showed resistance, no IC$_{50}$		6% @ 500 nM	255.2	230 nM	ND	incomplete	[11]
								ND	incomplete	
gemcitabine	Capan-1	3D	showed resistance, no IC$_{50}$		25% @ 500 nM	231.4	63 nM	1.00	partial	
docetaxel	MDA-MB-231	3D	IC$_{50}$ = 10 μM		29% @ 0.1 μM	312.4	could not determine	0.88	incomplete	[34]

Table 3. IC_{50} reported in a publication differed from that calculated by our laboratory independently.

| drug | cell line | format | reported IC_{50} | calculated | | | | | | curve | group |
				IC_{50}	E_{max} (growth inhibition)	AUC	EC_{50}	R^2		
paclitaxel	SPCA-1	3D	2.97 μM	7.9 μM	84% @ 8.5 μM	19.7	7.75 μM	0.99	incomplete	[36]
	786-0	2D	38.0–51.3 μM	782 μM	62% @ 0.1 μM	212.20	0.04 μM	0.97	partial	[18]
	SW620	2D	2.6–3.6 μM	0.006 μM	100% @ 0.2 μM	128.70	0.006 μM	0.95	partial	
	HT29	2D	2.8–4.7 μM	0.003 μM	100% @ 0.2 μM	119.20	0.003 μM	0.96	partial	
	HeLa	2D	2.3–7.4 μM	0.02 μM	98% @ 0.1 μM	372.00	0.008 μM	0.99	partial	
	SY5Y	2D	1.7–2.0 μM	0.006 μM	94% @ 0.1 μM	377.10	0.005 μM	0.99	partial	
	PC3	2D	12.9–13.0 μM	0.03 μM	100% @ 0.2 μM	159.90	0.02 μM	0.99	partial	
doxorubicin	HEPG2 (cocultured with LX-2)	3D	50.4 μM	24.5 μM	69% @ 1957 μM	341.20	17.6 μM	0.99	partial	[37]
doxorubicin	HEPG2 (cocultured with LX-2)	2D	33.1 μM	228.7 μM	99% @ 213 μM	421.90	27.4 μM	0.89	partial	
doxorubicin + 0.1 μM calcipotriol	HEPG2 (cocultured with LX-2)	3D	6.9 μM	3.92 μM	76% @ 1660 μM	317.10	5.89 μM	0.92	partial	
doxorubicin + 0.1 μM calcipotriol	HEPG2 (cocultured with LX-2)	2D	43.7 μM	624.8 μM	96% @ 225 μM	388.40	42.7 μM	0.96	partial	
epirubicin	MCF7	3D	0.5 μM	9.1 μM	98% @ 196 μM	406.30	3.8 μM	0.96	partial	[21]
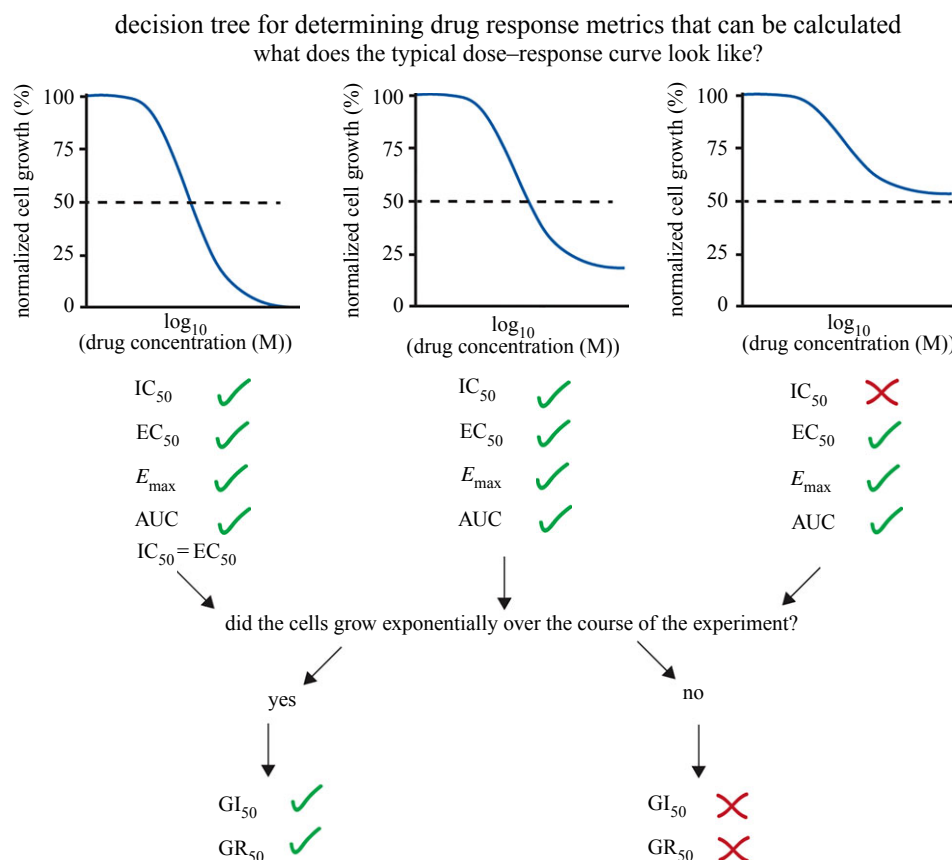
Figure 3. Decision tree for determining what drug response metrics can be calculated from drug response data. It is easiest to first look at a typical dose-response curve and calculate data from it. Then, depending on cell growth over the course of the assay, additional metrics may be calculated. In the first step, the criterion is whether the normalized cell growth decreased below 0.5, which is required for IC_{50} calculation. Criterion for the second step is whether exponential growth was achieved during the experiment. (Online version in colour.)

recently shown that basal-like and mesenchymal-like sub-classes of breast cancer could be distinguished based on their expected drug sensitivities, but only when cocultured with fibroblasts [41]. It is unclear how much complexity is required to accurately predict *in vivo* drug efficacy, but recreating aspects of the cellular TME is emerging as an important consideration due to the *in vivo* spatial heterogeneity. Logsdon *et al.* [40] found that MDA-MB-231 cells in mixed, 3D culture with fibroblasts were more resistant to 10 μM doxorubicin at low ratios of tumour to stromal cells (4 : 1) but equally affected by the drug at higher ratios (1 : 4). Shen *et al.* [45] found similar results using a micropatterned interface of tumour to stromal cells wherein MCF7 cell proliferation was inhibited by reversine at the interface but not in the bulk. Expanding these datasets to evaluate a range of drug doses would provide insight into how dose response varies between the tumour bulk and regions of more diffuse invasion.

One challenge with cocultures is the determination of drug response metrics for the discrete populations of cells. It is easiest to use cells expressing a reporter transgene or labelled with non-toxic dyes. Measurement of total fluorescence or bioluminescence then provides an estimate of the labelled cell number over the course of drug treatment [46,47]. However, dead cells may remain within 3D models, so the use of total fluorescence readings in these systems may be inaccurate. More appropriate in 3D is to stain cells using a viability marker like propidium iodide or JC-1 and quantify cell viability and/or number using either confocal/multiphoton microscopy or flow cytometry [40,41,44].

These methods can be used to track the drug response of one cell type while ignoring other cell types, or examine it for multiple cell types via multiplexing of different fluorophores. Coculture systems do require deciding which sample is more appropriate for calculating y_{ctrl}: a cancer cell only sample or a sample with all the cell types. Arguably, the respective untreated sample should be used for each treated sample to compensate for any effects of the stromal cells on cancer cell viability or growth rate. Additionally, the multiple centrifugation steps involved in harvesting and labelling cells for flow cytometry carry a risk of decreasing cell yield, such that it would be best to seed separate samples at the start of the study for determining an accurate y_0.

Physically separating stromal and tumour cells using either conditioned media or culture inserts can isolate effects, but several studies have shown that direct cell–cell contact may be a crucial component of stromal-derived effects on cancer cells [45,48,49]. In mixed cultures, the most common methods to assess cell viability, such as MTT assay, Alamar-Blue and CellTiter-Glo, measure the entire population of cells such that isolating the effects on only the cancer cells is not feasible. For example, by using CellTiter-Glo, Ngo & Harley [25] reported an increase in the overall growth rate of glioblastoma–endothelial cell cocultures with increasing temozolomide concentration, but it is unknown if both cell types contributed equally. It is possible the cancer cells responded the same as in monoculture (growth rate inhibition), while endothelial cells increased their growth rate, or that only endothelial cells were affected and therefore protected the cancer cells. Separating the responses of different

cell types may not always be a significant drawback, but the presence of stromal cells has the potential to confound the results if overall survival apparently increases with drug treatment, as was reported by Yang *et al.* [46], such that IC_{50} or EC_{50} would be impossible to calculate. Thus, it may be more appropriate in these multicellular cultures to calculate GR_{50} or GI_{50} to determine overall drug responses across conditions.

6. Conclusion

Drug screening in biomaterials could be particularly useful in making better predictions in the early stages of preclinical drug development. However, it can be challenging to compare drug responses across different platforms and conditions in the current literature. This is, in part, a result of inconsistent applications of drug response metrics, and differences in cell growth rates for cells cultured in different biomaterials. For this reason, we suggest the use of GI_{50} and GR_{50} to account for initial populations (y_0) and number of cell divisions during an assay, since cell growth highly impacts dose response. However, in instances when steady cell growth is not achieved, multiple drug response metrics could be applied (e.g. IC_{50}, EC_{50}, E_{max} and AUC) to account for possible experimental variation. To aid researchers in determining what drug response metrics can be calculated from their data, we suggest the use of a decision tree (figure 3) based on the traditional drug response curve and cell growth rate data that are obtained for a drug response experiment. First, visual inspection of a drug response curve will determine if an IC_{50} can be calculated if less than 50% of the control cell population is remaining at the highest drug concentration that was tested. If 100% cell death has been achieved, then the EC_{50} and IC_{50} will be equal. Furthermore, if the cells grew exponentially over the course of the drug screening assay, then the GI_{50} and GR_{50} metrics can be applied. We also encourage other research groups to incorporate raw data and drug response curves in their reports that will allow other researchers to gather additional data for their analyses. In the long term, this will lead to more accurate predictions early in the drug development pipeline of how likely a drug will be successful in a clinical setting.

References

1. Hafner M, Niepel M, Chung M, Sorger PK. 2016 Growth rate inhibition metrics correct for confounders in measuring sensitivity to cancer drugs. *Nat. Methods* **13**, 521–527. (doi:10.1038/nmeth.3853).

2. Haibe-Kains B, El-Hachem N, Birkbak NJ, Jin AC, Beck AH, Aerts HJWL, Quackenbush J. 2013 Inconsistency in large pharmacogenomic studies. *Nature* **504**, 389–393. (doi:10.1038/nature12831).

3. Garnett MJ et al. 2012 Systematic identification of genomic markers of drug sensitivity in cancer cells. *Nature* **483**, 570–575. (doi:10.1038/nature11005).

4. Barretina J et al. 2012 The cancer cell line encyclopedia enables predictive modelling of anticancer drug sensitivity. *Nature* **483**, 603–307. (doi:10.1038/nature11003)

5. Gillies RJ, Didier N, Denton M. 1986 Determination of cell number in monolayer cultures. *Anal. Biochem.* **159**, 109–113. (doi:10.1016/0003-2697(86)90314-3)

6. Inglese J, Auld DS, Jadhav A, Johnson RL, Simeonov A, Yasgar A, Zheng W, Austin CP. 2006 Quantitative high-throughput screening: a titration-based approach that efficiently identifies biological activities in large chemical libraries. *Proc. Natl Acad. Sci USA* **103**, 11 473–11 478. (doi:10.1073/pnas.0604348103)

7. Marques J, Vilanova E, Mourao PAS, Fernandez-Busquets X. 2016 Marine organism sulfated polysaccharides exhibiting significant antimalarial activity and inhibition of red blood cell invasion by *Plasmodium*. *Sci. Rep.* **6**, 24 368. (doi:10.1038/srep24368)

8. Bulysheva AA, Bowlin GL, Petrova SP, Yeudall WA. 2013 Enhanced chemoresistance of squamous carcinoma cells grown in 3D cryogenic electrospun scaffolds. *Biomed. Mater.* **8**, 055009. (doi:10.1088/1748-6041/8/5/055009)

9. Fallahi-Sichani M, Honarnejad S, Heiser LM, Gray JW, Sorger PK. 2013 Metrics other than potency reveal systematic variation in responses to cancer drugs. *Nat. Chem. Biol.* **9**, 708–714. (doi:10.1038/nchembio.1337)

10. Sebaugh JL. 2011 Guidelines for accurate EC50/IC50 estimation. *Pharm. Stat.* **10**, 128–134. (doi:10.1002/pst.426)

11. Longati P et al. 2013 3D pancreatic carcinoma spheroids induce a matrix-rich, chemoresistant phenotype offering a better model for drug testing. *BMC Cancer* **13**, 95. (doi:10.1186/1471-2407-13-95)

12. Hongisto V, Jernstrom S, Fey V, Mpindi JP, Kleivi Sahlberg K, Kallioniemi O, Perala M. 2013 High-throughput 3D screening reveals differences in drug sensitivities between culture models of JIMT1 breast cancer cells. *PLoS ONE* **8**, e77232. (doi:10.1371/journal.pone.0077232)

13. Phan N, Hong JJ, Tofig B, Mapua M, Huang J, Memarzadeh S. 2018 A simple high-throughput approach to identify actionable drug responses in patient-derived tumor organoids. *bioRxiv*. (doi:10.1101/138412).

14. Monks A et al. 1991 Feasibility of a high-flux anticancer drug screen using a diverse panel of cultured human tumor cell lines. *J. Natl Cancer Inst.* **83**, 757–766. (doi:10.1093/jnci/83.11.757)

15. Valeriote FA, Corbett TH, Baker LH. 2012 Cytotoxic anticancer drugs: models and concepts for drug discovery and development. In *Proc. 22nd Annu. Cancer Symp., Detroit, Michigan, USA, 26–28 April 1990*, Berlin, Germany: Springer Science & Business Media.

16. Vinci M et al. 2012 Advances in establishment and analysis of three-dimensional tumor spheroid-based functional assays for target validation and drug evaluation. *BMC Biol.* **10**, 29. (doi:10.1186/1741-7007-10-29)

17. Lovitt CJ, Shelper TB, Avery VM. 2018 Doxorubicin resistance in breast cancer cells is mediated by extracellular matrix proteins. *BMC Cancer* **18**, 41. (doi:10.1186/s12885-017-3953-6).

18. Zustiak S, Nossal R, Sackett DL. 2014 Multiwell stiffness assay for the study of cell responsiveness to cytotoxic drugs. *Biotechnol. Bioeng.* **111**, 396–403. (doi:10.1002/bit.25097)

19. Mih JD, Sharif AS, Liu F, Marinkovic A, Symer MM, Daniel J. 2011 A multiwell platform for studying

12

royalsocietypublishing.org/journal/rstb Phil. Trans. R. Soc. B 374. 20180226

stiffness-dependent cell biology. *PLoS ONE* **6**, 1–10. (doi:10.1371/journal.pone.0019929)

20. Nguyen TV, Sleiman M, Moriarty T, Herrick WG, Peyton SR. 2014 Sorafenib resistance and JNK signaling in carcinoma during extracellular matrix stiffening. *Biomaterials* **35**, 5749–5759. (doi:10.1016/j.biomaterials.2014.03.058)

21. Lovitt CJ, Shelper TB, Avery VM. 2015 Evaluation of chemotherapeutics in a three-dimensional breast cancer model. *J. Cancer Res. Clin. Oncol.* **141**, 951–959. (doi:10.1007/s00432-015-1950-1)

22. Ivanov DP, Parker TL, Walker DA, Alexander C, Ashford MB, Gellert PR, Garnett MC. 2014 Multiplexing spheroid volume, resazurin and acid phosphatase viability assays for high-throughput screening of tumour spheroids and stem cell neurospheres. *PLoS ONE* **9**, 1–14. (doi:10.1371/journal.pone.0103817)

23. Baker BM, Chen CS. 2012 Deconstructing the third dimension—how 3D culture microenvironments alter cellular cues. *J. Cell Sci.* **125**, 3015–3024. (doi:10.1242/jcs.079509)

24. Hafner M, Heiser LM, Williams EH, Niepel M, Wang NJ, Korkola JE, Gray JW, Sorger PK. 2017 Quantification of sensitivity and resistance of breast cancer cell lines to anti-cancer drugs using GR metrics. *Sci. Data* **4**, 170166. (doi:10.1038/sdata.2017.166)

25. Ngo MT, Harley BAC. 2018 Perivascular signals alter global gene expression profile of glioblastoma and response to temozolomide in a gelatin hydrogel. *Biomaterials* **198**, 122–134. (doi:10.1016/j.biomaterials.2018.06.013)

26. Gencoglu MF, Barney LE, Hall CL, Brooks EA, Schwartz AD, Corbett DC, Stevens KR, Peyton SR. 2018 Comparative study of multicellular tumor spheroid formation methods and implications for drug screening. *ACS Biomater. Sci. Eng.* **4**, 410–420. (doi:10.1021/acsbiomaterials.7b00069)

27. Schwartz AD, Barney LE, Jansen LE, Nguyen TV, Hall CL, Meyer AS, Peyton SR. 2017 A biomaterial screening approach reveals microenvironmental mechanisms of drug resistance. *Integr. Biol.* **9**, 912–924. (doi:10.1039/c7ib00128b)

28. Bray LJ, Binner M, Holzheu A, Friedrichs J, Freudenberg U, Hutmacher DW, Werner, C. 2015 Multi-parametric hydrogels support 3D in vitro bioengineered microenvironment models of tumour angiogenesis. *Biomaterials* **53**, 609–620. (doi:10.1016/j.biomaterials.2015.02.124)

29. Talukdar S, Kundu SC. 2012 A non-mulberry silk fibroin protein based 3D in vitro tumor model for evaluation of anticancer drug activity. *Adv. Funct.*

Mater. **22**, 4778–4788. (doi:10.1002/adfm.201200375)

30. Gong X, Lin C, Cheng J, Su J, Zhao H, Liu T, Wen X, Zhao P. 2015 Generation of multicellular tumor spheroids with microwell-based agarose scaffolds for drug testing. *PLoS ONE* **10**, e0130348. (doi:10.1371/journal.pone.0130348)

31. Phan N, Tofig B, Huang J, Memarzadeh S, Damoiseaux R, Soragni A. 2017 Miniring approach for high-throughput drug screenings in 3D tumor models. *bioRxiv* 138412. (doi:10.1101/138412)

32. Ho WY, Yeap SK, Ho CL, Rahim RA, Alitheen NB. 2012 Development of multicellular tumor spheroid (MCTS) culture from breast cancer cell and a high throughput screening method using the MTT assay. *PLoS ONE* **7**, e44640. (doi:10.1371/journal.pone.0044640)

33. Sarkar J, Kumar A. 2016 Thermo-responsive polymer aided spheroid culture in cryogel based platform for high throughput drug screening. *Analyst* **141**, 2553–2567. (doi:10.1039/C6AN00356G)

34. Clémence D, Robin D, Pierre D, Corinne A, Claire S, Christelle B, Emmanuelle M, Frédérique P-L, Bamdad M. 2017 Development and cytotoxic response of two proliferative MDA-MB-231 and non-proliferative SUM1315 three-dimensional cell culture models of triple-negative basal-like breast cancer cell lines. *Oncotarget* **8**, 95316. (doi:10.18632/oncotarget.20517)

35. Ma W-Y, Hsiung L-C, Wang C-H, Chiang C-L, Lin C-H, Huang C-S, Wo AM. 2015 A novel 96well-formatted micro-gap plate enabling drug response profiling on primary tumour samples. *Sci. Rep.* **5**, 9656. (doi:10.1038/srep09656)

36. Xu Z, Gao Y, Hao Y, Li E, Wang Y, Zhang J, Wang W, Gao Z, Wang Q. 2013 Application of a microfluidic chip-based 3D co-culture to test drug sensitivity for individualized treatment of lung cancer. *Biomaterials* **34**, 4109–4117. (doi:10.1016/j.biomaterials.2013.02.045)

37. Zhu L. 2017 Biomechanically primed liver microtumor array as a high-throughput mechanopharmacological screening platform for stroma-reprogrammed combinatorial therapy. *Biomaterials* **124**, 12–24. (doi:10.1016/j.biomaterials.2017.01.030)

38. Mosmann T. 1983 Rapid colorimetric assay for cellular growth and survival: application to proliferation and cytotoxicity assays. *J. Immunol. Methods* **65**, 55–63. (doi:10.1016/0022-1759(83)90303-4)

39. Drevon D, Fursa SR, Malcolm AL. 2017 Intercoder reliability and validity of WebPlotDigitizer in extracting graphed data. *Behav. Modif.* **41**, 323–339. (doi:10.1177/0145445516673998)

40. Logsdon DK, Beeghly GF, Munson JM. 2017 Chemoprotection across the tumor border: cancer cell response to doxorubicin depends on stromal fibroblast ratios and interstitial therapeutic transport. *Cell. Mol. Bioeng.* **10**, 463–481. (doi:10.1007/s12195-017-0498-3)

41. Landry BD et al. 2018 Tumor-stroma interactions differentially alter drug sensitivity based on the origin of stromal cells. *Mol. Syst. Biol.* **14**, e8322. (doi:10.15252/msb.20188322)

42. Cardenas C, Montagna MK, Pitruzzello M, Lima E, Mor G, Alvero AB. 2017 Adipocyte microenvironment promotes Bclxl expression and confers chemoresistance in ovarian cancer cells. *Apoptosis* **22**, 558–569. (doi:10.1007/s10495-016-1339-x)

43. Duong MN, Cleret A, Matera EL, Chettab K, Mathe D, Valsesia-Wittmann S, Clemenceau B, Dumontet C. 2015 Adipose cells promote resistance of breast cancer cells to trastuzumab-mediated antibody-dependent cellular cytotoxicity. *Breast Cancer Res.* **17**, 57. (doi:10.1186/s13058-015-0569-0)

44. Harris AR, Yuan JX, Munson JM. 2018 Assessing multiparametric drug response in tissue engineered tumor microenvironment models. *Methods* **134**, 20–31. (doi:10.1016/j.ymeth.2017.12.010)

45. Shen K et al. 2014 Resolving cancer-stroma interfacial signalling and interventions with micropatterned tumour-stromal assays. *Nat. Commun.* **5**, 5662. (doi:10.1038/ncomms6662)

46. Yang N et al. 2014 A co-culture model with brain tumor-specific bioluminescence demonstrates astrocyte-induced drug resistance in glioblastoma. *J. Transl. Med.* **12**, 278. (doi:10.1186/s12967-014-0278-y)

47. Goliwas KF, Richter JR, Pruitt HC, Araysi LM, Anderson NR, Samant RS, Lobo-Ruppert SM, Berry JL, Frost AR 2017 Methods to evaluate cell growth, viability, and response to treatment in a tissue engineered breast cancer model. *Sci. Rep.* **7**, 14167. (doi:10.1038/s41598-017-14326-8)

48. Chen Q et al. 2016 Carcinoma-astrocyte gap junctions promote brain metastasis by cGAMP transfer. *Nature* **533**, 493–498. (doi:10.1038/nature18268)

49. Borovski T et al. 2009 Tumor microvasculature supports proliferation and expansion of glioma-propagating cells. *Int. J. Cancer* **125**, 1222–1230. (doi:10.1002/ijc.24408)